Comparison of Dynamic Characteristics of the Line Start Permanent Magnet Motor and the Induction Motor

Byoung Yull Yang, Byung Il Kwon, Chul Kyu Lee, Kyung Il Woo and Byung Taek Kim

Abstract - The line start permanent magnet (LSPM) motor has been developed facilitate to the design of the synchronous motor. The rotor of this motor is composed of interior permanent magnets and aluminum bars instead of rotor windings. It is difficult to predict the performance characteristics accurately, because many characteristics are produced by the aluminum rotor bars and the permanent magnets. Therefore, in this paper the dynamic characteristics of the LSPM motor are described and compared via the time-stepped finite element method with those of the cage-type induction motor to find the characteristics of the permanent magnets and the rotor bars in the LSPM motor

Keyword - finite element method, induction motor, interior permanent magnet, line start motor

1. Introduction

A permanent magnet synchronous motor has good performance and high efficiency, it has no starting torque, so a driving system for starting Comparison of Dynamic Characteristics of the Line Start Permanent Magnet Motor and the Induction Motor is needed. There are two starting methods of the line start permanent magnet (LSPM) motor : the induction type motor that is started by the auxiliary windings like the wound-rotor type induction motor and the inverter-driven type motor that is started by the external inverter system. However, realizing the two starting methods studies is very difficult.

In recent, a permanent magnet synchronous motor with aluminum bars in the rotor, that is, an LSPM motor, is developed to avoid starting system complexity[1~5]. But, the characteristics using equivalent circuit method to analyze of the LSPM motor, because many characteristics are produced by aluminum rotor bars and permanent magnets. The finite element method should be used to analyze the characteristics of the LSPM motor.

The radial length of the permanent magnet affect its characteristics[6]. In this paper, we kept the width of the permanent magnet and varied its radial length, as shown in Fig. 1, for convenience of analysis. In other words, by varying the radial length of the permanent magnet of the LSPM motor, are analyzed in advance the characteristics for choosing the size of the permanent magnet. Then the dynamic characteristics of the LSPM motor and the induction motor are compared to determine the characteristics of the permanent magnets and the rotor bars in the LSPM motor. As a result, the dynamic characteristics, such as, speed, torque, and eddy current, of the LSPM are compared with those of the general induction motor. Therefore, the purpose of this paper is to use the time-stepped element method to compare the dynamic characteristics of the LSPM motor with those of the general induction motor.

This work was surpported by the research fund of Hanyang University(HY-2001-G)

Manuscript received: Dec. 12, 2001 accepted: Aug. 26, 2002

Byoung Yull Yang, Byung Il Kwon, and Chul Kyu Lee are with the Department of Electronic, Electrical Control, and Instrumentation Engineering, Hanyang University, Ansan, 425-791, Korea.

Kyung Il Woo is with the Department of Electrical, Control, and Instrument Engineering, Pukyong National University, Busan, Korea.

Byung Taek Kim is a senior researcher of Digital Appliance Lab, LG Electronics, 327-23, Gasan-dong, Kumchun-ku, Seoul, Korea.

2. Analysis Models And Finite Element Method

2.1 Analysis Models

Figs. 1 (a) and (b) show the 1/4 analysis models of the 3.75 kW general induction motor and the LSPM motor, which has a stator and a rotor in the same dimension of the general induction motor. Four permanent magnets (NdFeB) and the rotor bars (aluminium) are buried in the rotor of the LSPM motor. In Fig. 1 (b), the shape of aluminium bar A is used to prevent the leakage flux produced by the permanent magnets. The LSPM motor

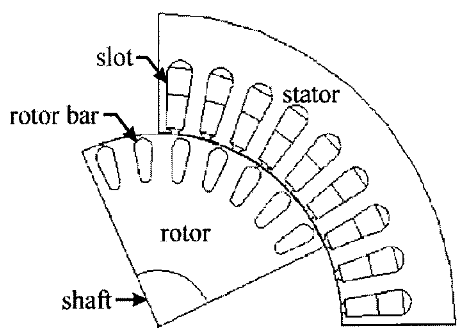

(a) The induction motor.

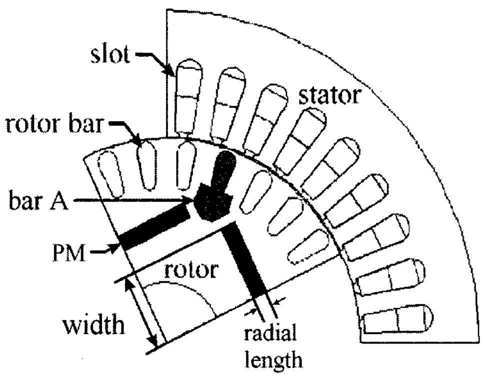

(b) The LSPM motor.
Fig. 1 Analysis models.

Table 1 Specification of the motor

Stator	Number of slots	36
	Number of poles	4 pole
	1 phase resistance	0.2 ohm
	Number of coil turns	96 turns
	Thickness	110 mm
	Material type	D23
Rotor	Air gap	0.3 mm
	Number of slots	28
	Permanent magnet	NdFeB
	Diameter of rotor	58 mm
	Thickness	110 mm
	Material type	D23
Characteristics	Output power	3.75 kW
	Input voltage	220 V
	Load torque	20 Nm
	Frequency	60 Hz

receives starting torque from the induced currents in the rotor bars before reaching synchronous speed. When it reaches the synchronous speed, the currents in the rotor bars vanish and the motor operates synchronously. Table I presents specifications of the induction motor and the LSPM motor. The residual flux density of the permanent magnet is 1.2 T.

2.2 Finite Element Method

The two-dimensional governing equation using magnetic vector potential A for the analysis model in Fig. 1 can be expressed as [7],

$$\frac{\partial}{\partial x}\left(\frac{1}{\mu}\frac{\partial A}{\partial x}\right)+\frac{\partial}{\partial y}\left(\frac{1}{\mu}\frac{\partial A}{\partial y}\right) = +\frac{N}{S}I_u-\frac{N}{S}I_v-\frac{N}{S}I_w -\frac{1}{\mu}\left(\frac{\partial M_y}{\partial x}-\frac{\partial M_x}{\partial y}\right)-\sigma\left(\frac{\partial A}{\partial t}+\nabla\phi\right). \quad (1)$$

Magnetic force densities acting on the rotor surface are calculated by the Maxwell stress tensor expressed as

$$t_n=\frac{1}{2\mu}(B_n^2-B_s^2) \quad [N/m^2] \quad (2)$$

$$t_s=\frac{B_n B_s}{\mu} \quad [N/m^2] \quad (3)$$

where t_n and t_s are normal and shear stress acting on the rotor surface and B_n and B_s are normal and tangential component of flux density going through the incremental area. Cogging torque and torque pulsation due to current ripple are calculated by

$$T=r\sum_{i=1}^{u}\frac{1}{\mu}[\overline{B_n^{(i)}}\,\overline{B_s^{(i)}}](D) \quad [Nm] \quad (4)$$

where u is the number of integration path on the rotor surface, r is the rotor radius, D is stator core length, and $\overline{B}_n$ and $\overline{B}_s$ are the normal and the shear component of average flux density on the integral path.

3. Simulation Results

3.1 Choice of the Permanent Magnet Size

Generally, the magnet size of the LSPM motor affects the motor's characteristics. For convenience of analysis, we kept the width of the permanent magnet and varied the radial length of the permanent magnet in the LSPM motor. To choose the permanent magnet size, the radial lengths of the permanent magnet are voluntarily chosen like Table II. The simulation conditions are 220 V, 60 Hz and load torque of 20 Nm. In Table 2, the power factors and the efficiencies of the LSPM motors with different magnet sizes are shown. According to Table 2, the efficiency of the LSPM motor with the permanent magnet radial length of 4.5 mm is best.

Table 2 Efficiency and power factor of the LSPM motor

The radial length of the magnet	The radial length of the magnet / The radius of the rotor	Power factor	Efficiency [%]
3.44	1/17	0.848	88.86
3.89	1/15	0.862	89.52
4.5	**1/13**	**0.879**	**90.38**
5.31	1/11	0.902	89.42
6.49	1/9	0.918	89.25

Fig. 2 shows the current characteristics of LSPM motors with different magnet sizes. In Fig. 2, the current amplitude of the LSPM motor with permanent magnet radial length of 6.49 mm is smallest. According to Table II, the LSPM motor with a 6.49 mm magnet is best in the power factor characteristics but less efficient because of the leakage fluxes. The longer the radial length of the permanent magnet, the more leakage fluxes. Therefore, a permanent magnet radial length of 4.5 mm is a moderate choice.

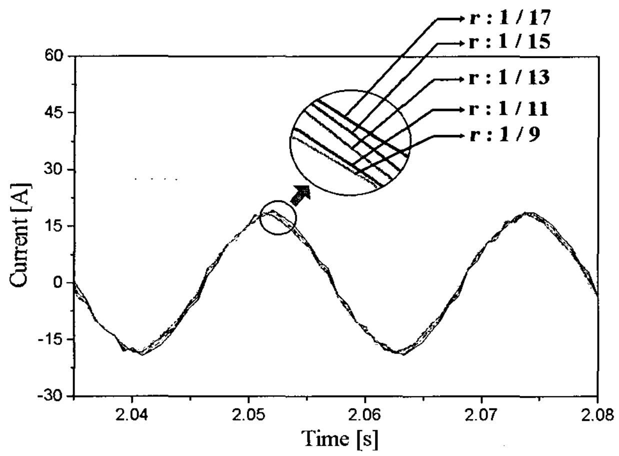

Fig. 2 Current waveform with different magnet sizes of the LSPM motors.

Figs. 3 (a) and (b) show the flux plots of the two types LSPM motors with 4.5 mm and 6.49 mm magnets at steady state. Fig. 3 shows that more leakage fluxes occur in Fig. 3 (b) : around A of Fig. 1 (b) : than in Fig. 3 (a).

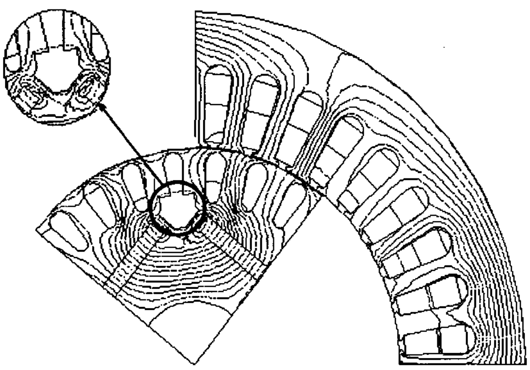

(a) The radial length of the permanent magnet of the LSPM motor is 4.5 mm.

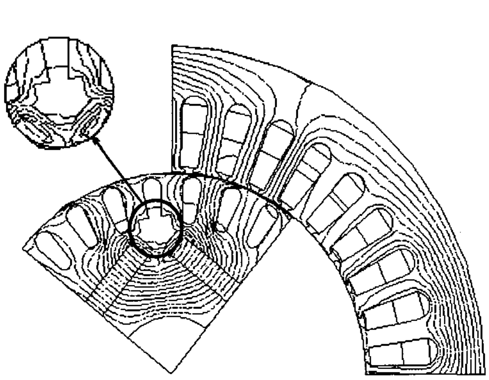

(b) The radial length of the permanent magnet of the LSPM motor is 6.49 mm.

Fig. 3 Flux plots of the LSPM motors at steady state.

3.2 Dynamic Characteristics of the LSPM Motor and Induction Motor

To find the characteristics of the permanent magnets and the rotor bars in the LSPM motor, the dynamic characteristics of the LSPM motor are compared with those of the induction motor. Fig. 4 and Fig. 5 show speed and torque, respectively, of the selected LSPM motor before and the induction motor, respectively. In Fig. 4, once the permanent magnets are introduced to the LSPM motor, significantly more torque ripples occur both during the transient state and the steady state due to the cogging torque produced by the permanent magnet. Comparing the peak LSPM motor speed with the peak, speed, induction motor, we can see an increase for the induction motor. The damping action of the rotor cage quickly acts to reduce these speed oscillations, and the motor settles down to synchronous speed quite quickly. Fig. 6 represents the eddy current in the rotor bars, and shows that eddy current of the LSPM motor is smaller than that of the induction motor during the starting period because the flux linkages produced by the stator current are interfered with the flux linkages produced by the permanent magnet. Table III shows the power factor and the efficiency of the selected LSPM motor and the induction motor. Table III illustrates that the power factor and the efficiency of the selected LSPM motor are greater than those of the induction motor.

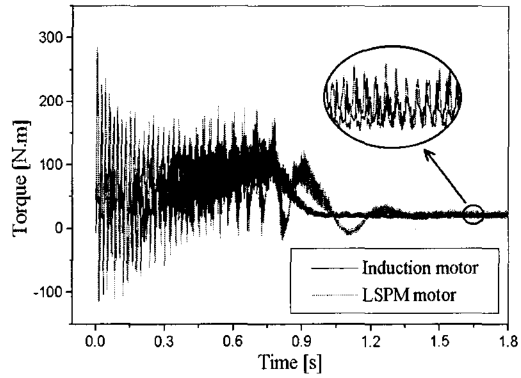

Fig. 4 Characteristics of the torque.

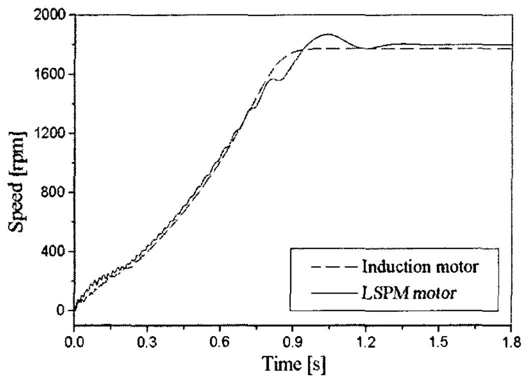

Fig. 5 Characteristics of the speed.

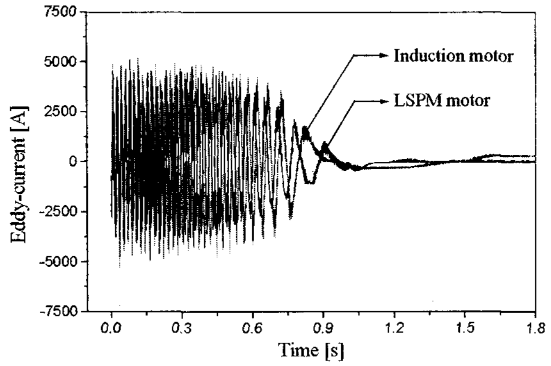

Fig. 6 Characteristics of the eddy current.

Table 3 Characteristic comparison of the LSPM motor and induction motor

	Power factor	Efficiency [%]
LSPM motor	0.879	**90.38**
Induction motor	0.854	**86.87**

4. Conclusions

This paper describes a comparison of dynamic characteristics of the line start permanent magnet motor and the induction motor. Simulation results indicate that the LSPM motor has more torque ripples during the transient state and the steady state than the induction motor due to cogging torque produced by the permanent magnets. The peak LSPM motor speed is greater than that of the induction motor. In addition, the eddy current of the LSPM motor is smaller than that of the induction motor during the starting period, and the efficiency and the power factor of the LSPM motor are better than that of the induction motor.

Acknowledgment

This work was supported by the research fund of Hanyang University (HY-2001-G).

Reference

[1] E. S. Hamdi, *Design of Small Electrical Machines*, John Wiley & Sons, 1990.

[2] E. Richter and T. W. Neumann, "Line start permanent magnet motors with different materials", *IEEE Trans. on Magnetics*, vol. MAG20, no. 5, pp. 1762~1764, Sept., 1984.

[3] N. Sadowski, S. R. Arruda, C. A. Da Silva, and L. Von Dokonal, "Single-phase line-satrted permanent magnet motor analysis using finite element method" *Industry Application Society Annual Meeting*, vol. 1, pp. 227~233, Oct., 1994.

[4] A. M. Knight, T. G. Salmoon, "Modeling the dynamic behavior of single-phase line-start permanent magnet motors", *IEEE Trans. on Industry Applications Conference*, vol. 4, pp. 2582~2588, Oct., 1999.

[5] A. M. Knight, and C. I. Mc Clay, "The design of high efficiency line-start motors", *IEEE Trans. on Industry Application*, vol. 36, no. 6, pp. 1555~11562, Nov./Dec., 1999.

[6] M. A. Rahman, and A. M. Osheiba, "Performance of large line-start permanent magnet synchronous motors", *IEEE Trans. on Energy Conversion*, vol. 5, no. 1, pp. 211~217, March, 1990.

[7] B. I. Kwon, K. I. Woo, D. J. Kim, and C. S. Park, "Finite element analysis for dynamic characteristics of an inverter-fed PMLSM by a new moving mesh technique", *IEEE Trans. on Magnetics*. vol. 36, no. 4, pp. 1574~1577, July 2000.

Byoung-Yull Yang was born in Namwon, Korea, on June. 21, 1973. He received the B.S. and M.S. degrees in Electrical Engineering from Hanyang University, Seoul, Korea, in 1999 and 2001, respectively. He is currently working toward the Ph.D. degree in the Department of Electronic, Electrical, Control, and Instrumentation Engineering, Hanyang University. His research interests include permanent magnet Motors (BLDC motors, and LSPM motors) and modeling transient phenomena with the finite-element method.

Byung Il Kwon was born in Andong, Korea, in February, 1956. He received the B.S. and M.S. degrees in electrical engineering from Hanyang University, Korea, in 1981, and 1983, respectively and Ph.D. degree in Electrical Engineering from Tokyo University, Japan, in 1989. He worked as a researcher at Toshiba System Software Laboratory in 1990 and as a senior researcher at Korea Institute of Industrial Technology in 1991. Since 1991, he has been on the faculty of Hanyang University. He served as a visit professor at University of Wisconsin-Madison in 2001. His research interests are linear drive systems, numerical analysis of electric machines, and control.

Chul-Kyu Lee was born in Kongju, Korea, on January 4, 1973. He received the B.S. and M.S. degrees in Electrical Engineering from Hanyang University, Seoul, Korea, in 1995 and 2001, respectively. He is currently working toward the Ph.D. degree in the Department of Electronic, Electrical, Control, and Instrumentation Engineering, Hanyang University. His research interests include permanent magnet motors, high efficiency motors, and modeling transient phenomena with the finite-element method.

Kyung il Woo was born in Korea in 1969. He received the B.S., M.S., and Ph.D. degrees in Electrical Engineering from Hanyang University in 1995, 1997 and 2001, respectively. He is currently a full-time instructor of the Division of Electrical, Control and Instrument Engineering of Pukyong National University, Busan. His research interests include electrical machine analysis and control. He is a member of KIEE and IEEE.

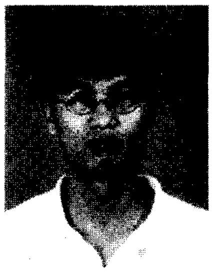

Byung-Taek Kim received the B.S., M.S., and Ph.D. degrees in Electrical Engineering from Hanyang University, Korea, in 1994, 1996, and 2001, respectively. He is working as a senior researcher of the Digital Appliance Lab at LG Electronics. His research interests include design of electric machines, numerical analysis, and optimization.